# Bestimmung des Ladezustands von Lithium-Ionen-Batterien mit geführten Wellen und Impedanzspektroskopie

Tobias GAUL [1], Konrad CHWELATIUK [1], Lars SCHUBERT [1]
[1] Fraunhofer IKTS, Fraunhofer Institut für keramische Technologien und Systeme, Dresden

Kontakt E-Mail: tobias.gaul@ikts.fraunhofer.de

**Kurzfassung.** Die Anwendung von Lithium-Ionen-Batterien ist heute weit verbreitet. Eine hohe verfügbare Leistung und Energiedichte machen sie neben Anwendungen in der Unterhaltungselektronik auch im rasch wachsenden Bereich der Elektromobilität interessant. Dabei ist für ihren effektiven Betrieb die Verfügbarkeit dieser Leistung über ihre gesamte Lebensdauer entscheidend. Ein Austausch des Akkus wird empfohlen, wenn die Kapazität durch Alterung auf unter 80% der ursprünglichen Kapazität gesunken ist. Für die Abschätzung der verbleibenden Zellenlebensdauer und die Optimierung der Einsatzzeit ist eine genaue Messung des Ladezustands (engl. state-of-charge, SoC) und der Restkapazität (engl. state-of-health, SoH) erforderlich. Dies kann auf Zellebene nicht durch herkömmliche Batteriemanagementsysteme gewährleistet werden, die nur auf Strom- und Spannungsmessungen beruhen.

Diese Arbeit stellt das Potential zur Bestimmung des SoC von Lithium-Ionen-Zellen mit elastisch geführten Wellen dar. Da die Wellenausbreitung von der Dichte und dem Elastizitätsmodul eines Mediums abhängig ist, kann eine Korrelation zwischen dem Ladezustand und der gemessenen Amplitude und Phase gezeigt werden, da sich die Porosität der Anode während des Ladens und Entladens ändert. In einer experimentellen Studie an einer repräsentativen Pouch-Zelle wurden mit piezoelektrischen Wandlern Sende-Empfangs-Messungen durchgeführt. Das verwendete Wandlernetzwerk ermöglicht dabei die Untersuchung unterschiedlicher Ausbreitungswege durch die Batterie.

Neben den Sende-Empfangs-Messungen zwischen zwei räumlich getrennten Wandlern wurde exemplarisch an einem Wandler eine Impedanzspetroskopie während des Ladeprozesses durchgeführt. Durch die Interaktion des Wandlers mit seiner Umgebung beinhaltet die Impedanzspetroskopie neben dem Verhalten des Wandlers auch die Änderungen an der Batteriezelle. Dabei werden unterschiedliche Messgrößen und Frequenzbereiche auf mögliche Effekte, durch die das Laden und Entladen der Batterie, hin untersucht. Abschließend werden beide Verfahren zur Ladezustandsüberwachung gegenübergestellt.

## 1. Introduction

The application of lithium-ion batteries (LIBs) is nowadays widespread. They can be found especially in consumer electronics such as mobile phones and notebooks, as well as in the rapidly growing field of electric cars. The highly available power and energy density of lithium-ion batteries over their lifetime are crucial for effective operation. However, their complex physicochemical nature should be more investigated, especially in the field of batteries' degradation. Degradation of the battery may occur over time and with use over several cycles and it can significantly reduce the battery's lifetime, which may have serious, dangerous effects for the user, e.g. while driving the electric vehicle. The main problems are the decrease in the LIB capacity and the decrease in power. The first is related to the amount of energy that can be stored in the LIB, the latter with the power that LIB can provide. In the process of LIB aging, these two problems may occur simultaneously [1].

To maintain a secure and effective operation of LIB they need to be monitored constantly. This is done with an additional Battery management system (BMS). The main task of the BMS is the constant monitoring of cell voltage, cell current, and cell temperature to avoid unwanted states, which could lead to the destruction of the LIB during operation. Besides, modern BMS estimates state-of-charge (SoC) and state-of-health (SoH) out of the monitored values. Besides the electrical parameters measured by the BMS also methods that rely on mechanical parameters can be used to determine the SoC and the SoH, as it is reviewed by Popp et al. [2]. Four possibilities were described in more detail by the authors. These methods are expansion-based methods, which measure the expansion and shrinking of a LIB during operation, experimental modal analysis, which measures damping and mode shapes during operation, ultrasonic measurements, which measures the change in elastic modulus of the anode and cathode and acoustic emission, which measures AE sources which are related with various degradation mechanisms.

Especially the use of ultrasonic measurements to characterize the state of modern lithium-ion batteries is addressed by different research groups due to their potential to determine the charge state and monitor the health state of a battery over the entire lifetime [3, 4, 5, 6].

One of the first works on this new research area was published by Sood et al. [7]. Monitoring is performed using a separate ultrasonic pulser and receiver that are attached to the external surfaces of a lithium-ion cell. Compressional waves were excited to verify the degradation of LIB's due to gas evolution. Real-time data from the ultrasonic transducer and receiver are used to non-destructively evaluate the internal condition of vital interfaces inside the cell. Also, the results were verified with radiographic images of degraded cells.

With a comparable transducer arrangement, Hsieh et al. [5] investigated the charge and health state in commercially available lithium-ion and alkaline batteries. The behavior of the transmitted and reflected bulk-wave signal was related to the SoC and aging processes within the cells. The results demonstrate strong correlations between the SoC and the density distribution within a cell, as determined by the acoustic measurements. Furthermore, it was shown that the proposed analysis technique will work regardless of the battery's chemistry and form factor.

The work conducted by Gold et al. [4] also presented a method of SoC estimation based on ultrasound transmission but used a pulser-receiver setup. They extended this method by showing, that ultrasonic signals in the LIB are sensitive to changes in porosity of graphite anode during cycling. Those changes in porosity of the anode are caused by the lithiation of graphite, which varying level has a big impact and is correlated with the SoC of the battery. Gold et al. explained this correlation with Biot's theory for the propagation of waves in fluid-saturated porous media.

In comparison to the previous authors, Ladpli et al. used guided elastic waves instead of ultrasonic waves to determine the SoC and SoH of a LIB. Piezoelectric transducers were attached on the surface of a battery and cycling under constant ambient condition were utilized [8]. Ladpli et al. proved a strong correlation between changes in the time-of-flight and the signal amplitude resulting from shifts in the guided wave signals and the electrochemical charge-discharge cycling and aging. With the use of differential voltage and differential time-of-flight analysis, they were able to detect intercalation staging and phase transitioning in the LIB. Besides, an analytical model of the battery was generated and the nominal magnitude and range of experimental time-of-flight during cycling are validated [9].

The work presented in this paper will follow the approach of Ladpli et al. and guided elastic waves are used for examination of the LIB. Multiple used transducers allow the analysis and comparison of different travel paths of the guided waves. In addition, a novel approach uses electro-mechanical impedance spectroscopy of a piezoelectric transducer to determine the SoC of the LIB. In comparison to electrochemical impedance spectroscopy (EIS), no access to the battery contacts is required.

## 2. Battery measurements with active excited guided waves

### *2.1 Measurement set-up for pitch-catch measurements*

The experiments were performed on a commercially available lithium polymer battery. Compared to LIB, this type uses a polymer electrode instead of a liquid electrode. The negative electrode is made of graphite, while the positive electrode consists of lithium cobalt oxide. The used battery type has a capacity of 10.000 mAh in mint condition and dimensions of 150 mm x 50 mm x 10 mm. Four piezoelectric transducers P-876.SP1 of PI Ceramic were used for generation and excitation of guided elastic waves. They were attached by honey and pressed on the surface with low force clamps to avoid damages inside the battery. The experimental setup can be seen in Figure 1. During the measurements, the environmental conditions were kept constant with a temperature of 25 °C and a humidity of 50 % in a climate chamber. For driving the piezoelectric transducers and receiving the signals, the MAS 2 hardware platform was used. As excitation, a four cycled Hanning windowed tone burst at frequencies of 75 and 110 kHz was used. The peak-to-peak amplitude of the actuation signals varies in these frequencies between 67.5 V and 90 V. Each signal path was sampled with 5 MHz and every point was averaged 64 times. During the charge and discharge cycle, a measurement every 5 min was carried out. At a constant current of 2 A, the full charge lasted 5 h, resulting in a total of 60 measurements per cycle.

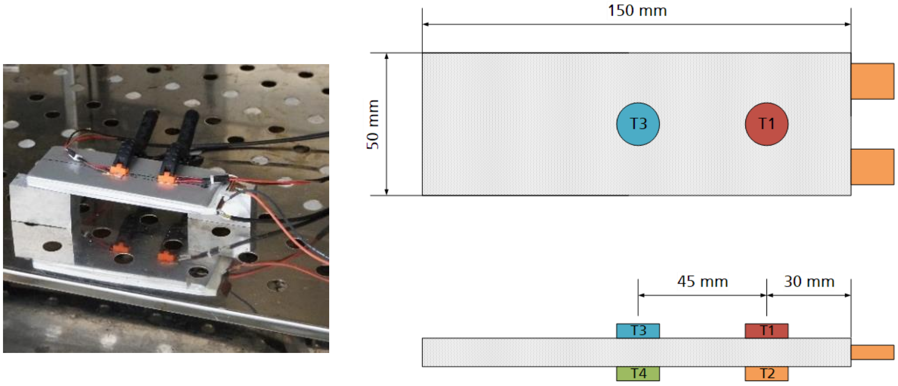


**Figure 1: Experimental setup in a climate chamber of Fraunhofer IKTS (left) and the arrangement of the four piezoelectric transducers on the battery (right)**

### *2.2 State of Charge estimation with pitch-catch measurements*

To illustrate the behavior of guided waves during charging and discharging of the battery, Figure 2 represents three signals of the transducer pair T3-T1 at different charge states during the charging phase. It can be seen that the signal amplitude of the received wave packages increases with an increasing state of charge. On the other hand, the wave package becomes more compact, resulting in a decreasing ToF while the SoC increases. For further analysis, the time-domain signal parameters maximum signal amplitude (SA) and time-of-flight (ToF) of the wave packet were extracted. To show the general behavior of guided waves during the charge and discharge process only the most sensitive path for each frequency is considered for further analysis in this paper.

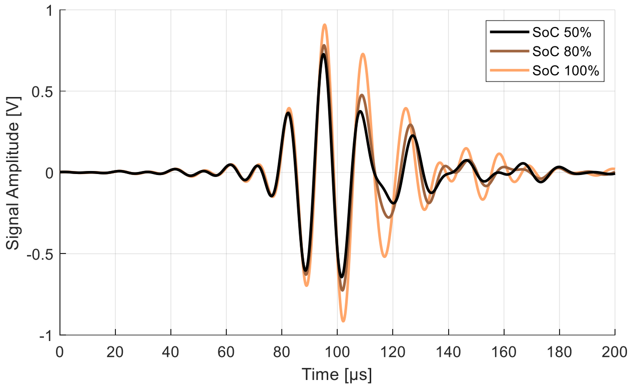


**Figure 2: Time-domain signals for transducer pair T3 (actuator) and T1 (sensor) at an excitation frequency of 75 kHz at different SoC level**

A signal path is supposed to be sensitive when the change in signal amplitude and time-of-flight is clearly visible within the data between charged and discharged state of the battery. Different configurations have their most sensitive change at different frequencies, whereas Path T3 – T1 is evaluated at 75 kHz and Path T3 – T2 is evaluated at 110 kHz.

The results of the time-domain signal parameters for the whole charge and discharge process at two different transducer configurations, T3 – T1 and T3 – T2 (compare Figure 1) at different frequencies are given in Figure 3(a) and (b). The results are plotted over the SoC where the actual battery capacity is normalized to the maximum charge capacity. For the transmission paths T3 – T1 and T3 – T2, there is a constant increase in SA and ToF above 30 % SoC in the charge phase and a constant decrease in the discharge phase. This is in accordance with other results from Hsieh et al. [5] where it was shown that during discharge, the acoustic absorption is generally increasing and therefore, the amplitude decreases. On contrary, the acoustic absorption is generally decreasing during charge, and therefore the amplitude increases. Below 30 % SoC the SA and ToF remain static or begin to shift in the opposite direction. In this range, the cell voltage drops below 3.5 V in the discharge phase and shows fast-changing values in the charge phase. Similar effects were observed by Ladpli et al. [8] in comparable measurements. In these ranges, it is hypothesized that an occurring phase transformation in the cathode leads to a strong change in the density and the modulus of the cathode [5]. When the cell is charged, the acoustic intensities decrease slightly as the phase transformation is reversed and then followed by a steady increase in the intensities with increasing SoC.

Another effect that can be recognized is a hysteresis between the charge and discharge cycle for both parameters ToF and SA. This is shown for the transducer pairs T3-T1 and T3-T2 in Figure 3(c) and (d) in detail, whereas the parameters of the charge cycles are plotted in solid lines and for the discharge cycle in dashed lines. In both plots, the parameters are normalized to their maximum value to avoid misinterpretation due to different absolute scale. For the two plots, both parameters show a comparable behavior, whereas in the discharge phase the measured parameters are larger than in the charge phase at comparable SoC levels. The curves for charging and discharging intersect between 30 % and 40 % SoC for the SA and between 10 % and 20 % for the ToF. Hysteresis effects has been reported before for both mechanical [10] and electrical [11] properties of lithium-ion cells. Roscher et al. compared the open-circuit voltage (OCV) and the SoC for the charge and discharge process [11]. They showed that the OCV after certain discharge steps is significantly lower than the OCV after charging and both curves enclose a hysteresis. The hysteresis was reduced with increasing current rate and it was stated out that interparticle charge transfer, resulting from strong inhomogeneities among the particles’ lithium contents, is a reasonable explanation for a shrinking OCV hysteresis with increasing current application. Sethuraman et al. reported of compressive stress due to binder swelling and electrochemical intercalation of lithium ions during charge and discharge process [10]. During deintercalation, the stress is reduced but also showed a hysteresis effect. In addition, there appears to be an approximate correlation between the rate of stress rise and the staging behavior of the lithiated graphite.

The previous authors also reported hysteresis effects and explained it with the different intercalation processes of lithium ions during charge and discharge within the anode. As the wave propagation of guided waves is also influenced by pre-stress within the material, hysteresis effects will appear in a comparable manner. The hysteresis will lead to uncertainties in the SoC determination when using one compensating curve for charging and discharging. The effect of hysteresis needs to be reviewed further to develop strategies for compensation.

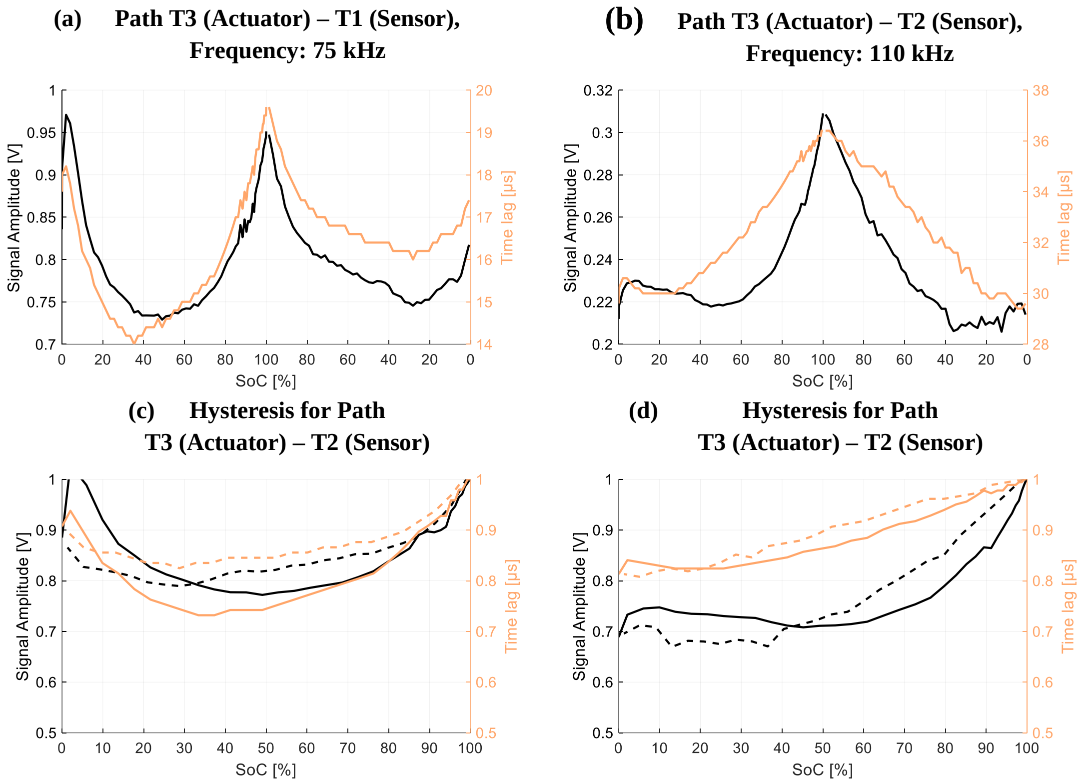


**Figure 3: Evolution of signal parameters ToF and SA with respect to the change in SoC for different transducer pairs (a) – (b) and hysteresis of signal parameters for the transducer pairs (c) - (d).**

## 3. Battery Measurement with Impedance spectroscopy

### *3.1 Measurement set-up*

The experiments were conducted with the same Lithium polymer battery used for the active guided wave measurements. Instead of four piezoelectric transducers, only one P-876.SP1 of PI Ceramic was used for the experiments. The transducer was placed on the surface in the center of the cell. Low force clamps ensured a constant pressure on the transducer which was coupled with honey. During the measurements, the impedance analyzer Keysight 4294A was connected by the sensing probe 42941A to the transducer and monitored its impedance periodically during subsequent cycles of charge and discharge of the battery. Impedance was measured every 5 minutes while the device excited the transducer. The excitation were conducted in the frequency range of 10 – 300 kHz, with a frequency step of 0,3625 kHz.

Each measurement point was averaged 4 times. Contrary to the pitch-catch measurement, the electromechanical impedance spectroscopy was not performed in a climate chamber. This time the experiment was conducted in standard conditions for temperature and pressure. Therefore, the temperature sensor was placed on the battery's surface. As in the pitch-catch measurement, the full charge took 5 h at a constant current of 2 A. The experimental setup is presented in Figure 4.

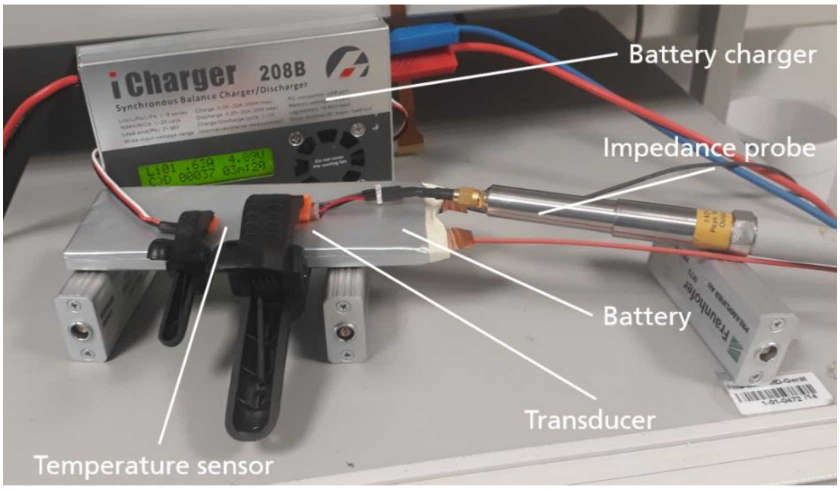


**Figure 4: Experimental setup for the electromechanical impedance spectroscopy**

### 3.2 *Results – SOC estimation in impedance spectroscopy*

To start the analysis of the impedance spectroscopy it is crucial to illustrate the values obtained experimentally. Out of 27 considered cycles, cycle 6$^{th}$ was taken for the analysis. Figure 5 a) shows the absolute values of impedance as a function of the excitation frequency and SoC in the charging phase. High amplitude of absolute impedance values is obtained for excitation frequencies below 10 kHz. At first sight, no conclusions can be drawn, except that the absolute impedance decreases with increasing excitation frequency, where the biggest span is in the frequency range up to ~20 kHz. The lack of any other visible correlations would mean, that it is difficult to indicate the SoC from the absolute impedance values only. However, the measurement of the impedance provides much more information about the behavior of the transducer e.g. phase angle, resistance or reactance. In Figure 5 b) the phase angle is presented as a function of the excitation frequency and SoC in the charging phase. In the frequency range between 160 and 220 kHz, a peak occurs which coincides with the resonance peak of the free oscillating transducer.

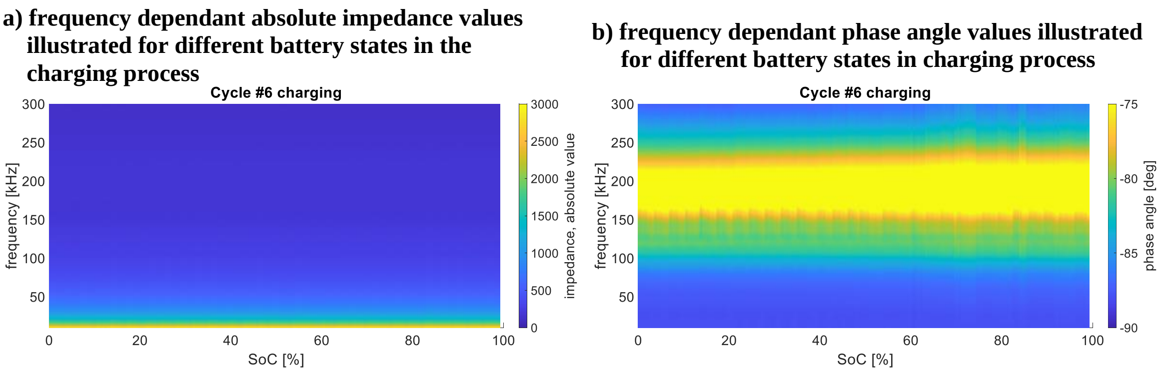


**Figure 5: Frequency dependant a) absolute impedance values and b) phase angle; illustrated for different battery states in charging phase**

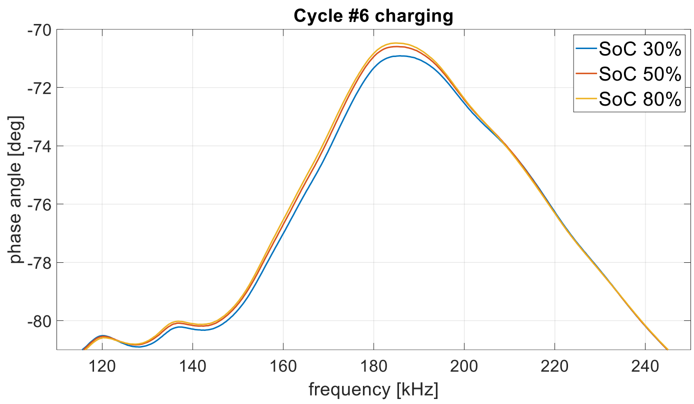

**Figure 6: Frequency-domain signals of phase angle at different SoC level in charging phase**

With increasing SoC a phase shift in the data can be identified what is assumed to accrue due to changing material parameters during the charging process. A detailed view of this behavior is presented in Figure 6. To show the effect of phase shift more clearly, the figure presents three different SoC states of the charging phase. It can be seen that the signals remain very similar, except in the frequency range between 170 and 200 kHz, where the signal amplitude increases with increasing SoC. This observation led to further analysis of changes between different SoC states.

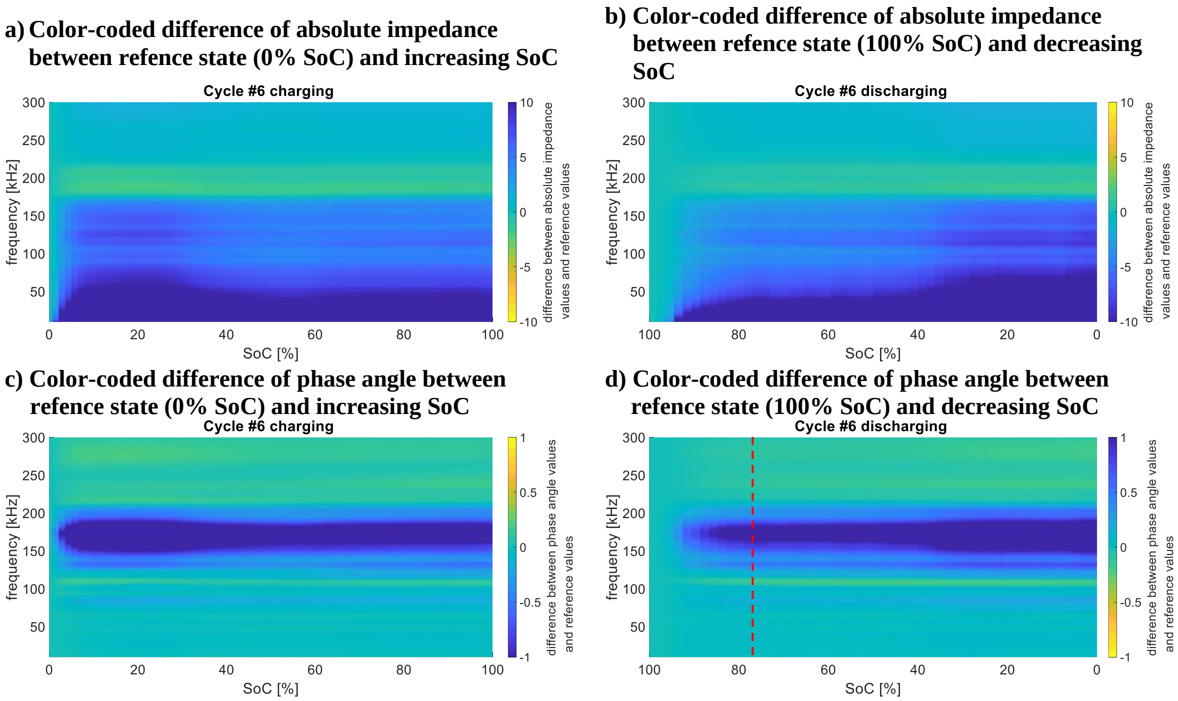

**Figure 7: Result of subtracting impedance a), b) and phase angle c), d) values in n-th SoC state and reference values for charging and discharging phase**

In further analysis, a baseline subtraction method was used to accentuate the differences in the data during charge and discharge. The reference point was chosen as 0 % or 100 %, the former for the charging phase, the latter for discharging phase. Then, values in this reference were subtracted from the values in each subsequent state, with the step of 1 %. This procedure was applied to both - absolute impedance and phase angle, what can be seen in Figure 7. For absolute impedance values in the charging phase (Figure 7 a)) it is evident that the differences increase in the range between 0-10 %, then saturates in the range between 10-30 %, and slightly decrease until 50 % and remain constant afterward. During the discharge phase (Figure 7 b)), it can be seen that differences are increasing in the range between 95-80 % and between 40-0 %. Besides the differences in impedance, Figure 7 c) and d) presents the differences in the phase angle for charging and discharging states. Moving towards the subsequent SoC states in the charging phase, the color-coded phase angle differences values are wider in SoC range 0-40 % and get narrower in the range 40-100 %. On the contrary, in the discharging phase, starting from 90 % up to 0 %, the differences are getting wider. Therefore, the phase angle of the EIS seems to be appropriate for the determination of the SoC.

To reduce the complexity of Figure 7 and to show how the EIS analysis may be used for SoC evaluation, the area under the curve for the difference values for each battery state was calculated to cover the entire frequency range – like it is presented in Figure 7 d), the sum of values on the red dotted line. Based on the chosen summation, primary the amplitude change of the phase angle is considered. Again, the step for every area calculation was equal to 1 % SoC. As a result, the obtained curves are presented in Figure 8 for the discharge phase for different battery cycles. During the discharge phase, the sum of phase angle difference is increasing constantly with decreasing SoC, except for the SoC range between 80 – 50 %, where the curves are flattened. In the range between 100 – 85 % a very rapid growth is observed, which may be explained by the phase instability of the cathode, where near 100 % state, a two-phase coexistence region occurs which may highly influence the properties of cathode [5]. Anyway, the line of the best fit would be linear for those curves, which could improve the SoC indication. Another thing, that can be observed in this graph, is that the amplitude of curves is decreasing along with an increasing number of cycles. Therefore, it can be concluded, that this type of analysis can be used not only for SoC indication, but also for SoH assessment. The SoH determination will be addressed in further work.

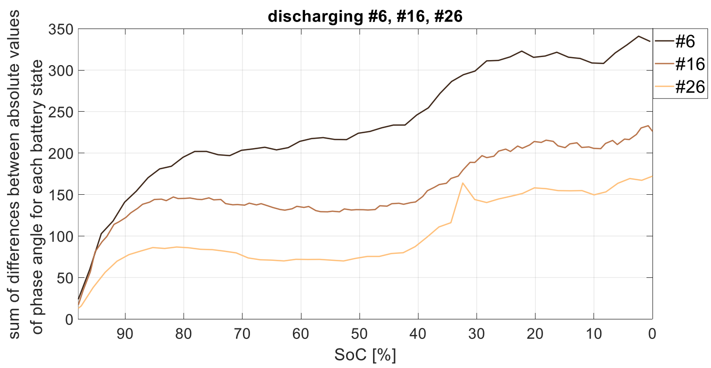


**Figure 8: Cumulative sum of differences of phase angle values in entire frequency range – discharging phase in cycle no. 6, 16 and 26**

## 4. Conclusion

The presented work shows the potential to determine the SoC of lithium-ion cells with different techniques using elastic guided waves and electromechanical impedance spectroscopy. For this purpose, extensive measurements with conventional surface-mounted piezoelectric transducers were performed on a commercially available Lithium polymer battery. Several signal parameters were used to show the correlation between the battery state and the change of the measured signal with both techniques.

In the first approach, multiple piezoelectric transducers were distributed on the surface of the battery. Guided waves were excited between the transducers and it was proven that all path combinations can measure a signal shift as a result of changing SoC in the battery. Therefore, the paper showed a clear dependence of SoC on signal amplitude and phase. However, the different pathways between the transducers have varying sensitivities at different frequencies. Also, a hysteresis between charge and discharge cycle for the chosen signal

parameters were encountered, which complicates the accurate determination of the SoC without further input data. It is hypothesized that different intercalation processes of lithium ions during charge and discharge within the anode are responsible for the hysteresis. As the hysteresis is also dependent on the present current, further work is needed to explain this phenomenon.
Another measurement method used for SoC determination was the electromechanical impedance spectroscopy. In comparison to active guided wave measurements, only one transducer is necessary to depict the correlation between SoC and the absolute values of the impedance spectroscopy. The paper showed, that in particular, the values related to the imaginary part of the impedance spectroscopy are sensitive to the change in SoC. Therefore, a baseline approach was introduced to consider the change of the phase in the whole measured frequency range and accentuate differences between the different battery states. This approach simplified the complete impedance spectrum to one value for every SoC step and is also capable to detect the ongoing loss of the capacity with an increasing amount of charge and discharge cycles. Further work will focus on the development of a monitoring strategy where SoC and SoH can be predicted simultaneously.

## References


[1] M. Woody, M. Arbabzadeh, G. M. Lewis, G. A. Keoleian und A. Stefanopoulou, „Strategies to limit degradation and maximize Li-ion battery service lifetime -Critical review and guidance for stakeholders,“ *Journal of Energy Storage,* 2020.

[2] H. Popp, M. Koller, M. Jahn und A. Bergmann, „Mechanical methods for state determination of Lithium-Ion secondary batteries: A review,“ *Journal of Energy Storage,* 2020.

[3] G. Davies, K. W. Knehr, B. Van Tassell, T. Hodson, S. Biswas, A. G. Hsieh und D. A. Steingart, „State of Charge and State of Health Estimation Using Electrochemical Acoustic Time of Flight Analysis,“ *Journal of The Electrochemical Society,* pp. 2746-2755, 2017.

[4] L. Gold, T. Bach, W. Virsik, A. Schmitt, J. Müller, T. E. M. Staab und G. Sextl, „Probing lithium-ion batteries' state-of-charge using ultrasonic transmission - Concept and laboratory testing,“ *Journal of Power Sources,* pp. 536-544, 2017.

[5] A. G. Hsieh, S. Bhadra, B. J. Hertzberg, P. J. Gjeltema, A. Goy, J. W. Fleischer und D. A. Steingart, „Electrochemical-acoustic time of flight: in operando correlation of physical dynamics with battery charge and health,“ *Energy & Environmental Science,* pp. 1569-1577, 2015.

[6] Y. Wu, Y. Wang, W. K. C. Yung und M. Pecht, „Ultrasonic Health Monitoring of Lithium-Ion Batteries,“ *Electronic,* 2019.

[7] B. Sood, O. Michael und P. Michael, „Health Monitoring of Lithium-ion Batteries,“ *IEEE Symposium,* 2013.

[8] P. Ladpli, F. Kopsaftopoulos, R. Nardari und F.-K. Chang, „Battery charge and health state monitoring via ultrasonic guided-wave-based methods using built-in piezoelectric transducers,“ *SPIE Smart Structures and Materials + Nondestructive Evaluation and Health Monitoring,* 2017.

[9] P. Ladpli, F. Kopsaftopoulos und F.-K. Chang, „Estimating state of charge and health of lithium-ion batteries with guided waves using built-in piezoelectric sensors/actuators,“ *Journal of Power Sources,* pp. 342-354, 2018.

[10] V. A. Sethuraman, N. Van Winkle, D. P. Abraham, A. F. Bower und P. R. Guduru, „Real-time stress measurements in lithium-ion battery negative-electrodes,“ *Journal of Power Sources,* pp. 334-342, 2012.

[11] M. A. Roscher, O. Bohlen und J. Vetter, „OCV Hysteresis in Li-Ion Batteries including Two-Phase TransitionMaterials,“ *International Journal of Electrochemistry,* pp. 1-6, 2011.